RSC Advances

ROYAL SOCIETY OF CHEMISTRY

www.rsc.org/advances

Graphical Abstract

The diffusion coefficient of Li^+ ions decreases with increase in LiCl concentration which depends on the size of coordination structure of ions formed in solutions.

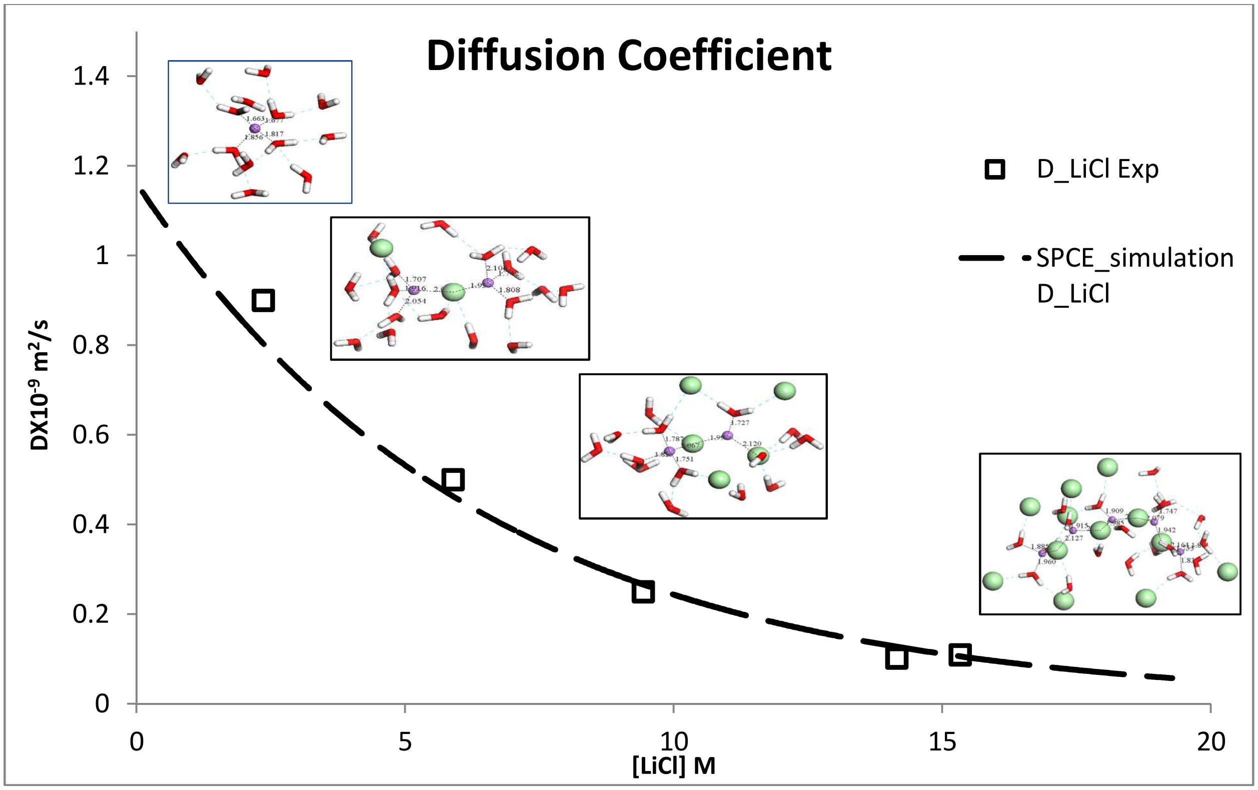

Investigations of Clustering of Ions and Diffusivity in Concentrated Aqueous Solutions of Lithium Chloride by Molecular Dynamic Simulation

Meena B. Singh, Vishwanath H. Dalvi, Vilas G. Gaikar*

Department of Chemical Engineering,
Institute of Chemical Technology,
Matunga, Mumbai – 400 019, India

*To whom correspondence should be addressed:

E-mail address: vg.gaikar@ictmumbai.edu.in

Tel.: +91 22 33612013,

Fax: +91 22 33611020;

Abstract

The interactions between lithium (Li^+) ions, chloride (Cl^-) ions and water molecules in aqueous LiCl solutions and their effect on the dynamic and equilibrium properties of the salt solutions have been investigated by molecular dynamics (MD) simulations. The optimized potentials for liquid simulations for all atoms (OPLS-AA) force field have been used to study various properties of lithium chloride solutions for the concentrations, in the range of 0.1M - 19.28 M. The MD simulation with the OPLS-AA force field gives a fair explanation of many important properties of alkali salt solutions which are in agreement with the experimental results. A microscopic description of LiCl solutions and diffusivity of LiCl obtained by simulation are in good agreement with the experimental data. The MD simulation indicated a strong solvation of monovalent ions in water and cluster formation of the cations at higher salt concentrations. The diffusion coefficient of LiCl decreases depending on the coordination structure of ions that changes with the salt concentration.

Key words: Molecular dynamics simulation; OPLS-AA force field; Salt solution; Coordination structure

1. Introduction

Investigating aqueous solutions of metal ions and ionic clusters has been an area of intensive scientific investigations for several decades.[1-4] The anions and cations of various alkali salt solutions, in particular, play an important role in nature, and therefore, experimental and theoretical studies of solvation of these monovalent ions have been done extensively.[5-8] The various properties of the alkali halide solutions, specifically diffusivity, solubility and viscosity have been studied as a function of concentration by both experimental and theoretical methods.[9,10] These studies reveal that the behavior of the metal ions is strongly decided by their size and charge density on the ions. Small metal ions, such as lithium, interact very strongly with water molecules that form a closely held and oriented hydrophilic shell around the metal ion while the larger metal ions show weaker interactions with the neighboring water molecules resulting in formation of a disoriented shell of water molecules around the ion. A macroscopic property of the aqueous solution depends on the alkali salt concentration which shows the effect of ions on the hydrogen bonding of water. The solvation shells of hydrated ions in aqueous solutions have been studied by various simulations[11-13] and experimental1[,14] techniques. Neutron scattering and X-ray diffraction experiments are done in past to study the solvation of water molecules around the ions, which proves that the structure of water gets affected by the cation-anion interactions[15-19].

Among alkali metal cations, Li^+ is the smallest ion having ionic radius of 0.059 nm[20] and bears the highest charge density of $1.86 \text{ X } 10^{11}$ C/m^3. On dissolution of lithium chloride in water, its dissociation and formation of lithium ions causes structural changes in its surrounding which are not observed in other single-charged alkali metal ions, due to which lithium salt solutions exhibit specific physicochemical features such as viscosity, diffusivity and solubility.[21] At infinitely dilute concentrations, it shows abnormal properties compared to chlorides of the other alkali metals.[22]

Among numerous papers concerning the hydration of alkali metal ions, a majority of the studies addresses the structural aspects of lithium salts in aqueous solutions because of their applications in chemical power sources and in part because of extremely high hygroscopic nature of the lithium halides.[22,23]

The energies of the *2s* and *2p* levels, in the ground state of Li, are very close. The energy of *2s* orbital is -520 kJ and that of *2p* is -340 kJ. Therefore, sp^3 hybridization arising from involvement of vacant *2s* and *2p* orbitals in the bonding with water molecules can be expected in complexes of lithium ions. The coordination number of a Li^+ ion is presumably determined by the type of hybridization of its vacant molecular orbitals and correspondingly, the presence of the fairly stable complex $Li(H_2O)_4^+$ in aqueous solutions was presumed.[23] Smirnov and Trostin[23] also mentioned that the formation of this complex is responsible for the abnormal properties of concentrated aqueous solutions of LiCl. In terms of the solution model, it was assumed that chloride ions replace the water molecules for a wide range of concentration of LiCl and form a tetrahedral surrounding of solvent molecules around Li^+ ions.[24] The solution properties are then decided by the presence of such complexes rather than individual ions in the solutions. The colligative properties of the solutions also are decided by the number of the ionic species and their sizes on dynamic time scale of the system.

Molecular Dynamics (MD) simulation is a powerful tool to study the materials at molecular level and extensively used to investigate; in particular, the aqueous solutions because of the highly hydrogen-bonded structure of water.[13,14] Many efforts have been made for the characterisation and optimization of energy parameters used for various alkali metal ions.[24,25]

MD studies are also useful for investigating the hydration and coordination structures of alkali metal ions such as Li^+, Na^+ and K^+[26]. But many of these MD studies are restricted to lower salt concentration range.[27,28] MD simulations have also been done to parameterize force field for various alkali metal ions.[24,29,30] While this work was on, Aragones *et al* [30] reported radial distribution functions of Li^+ and Cl^- ions in aqueous solutions of LiCl upto 10 M concentration, by using JC force field and TIP4P /2005 water model. These authors claimed that modified Lorentz- Berthelot (MLB) mixing rules were necessary to get the better fit of the simulated RDFs with the experimentally[31] estimated ion pairing parameters. However, we shall show in the present simulation that such a modification is not necessary, if appropriate force field parameters are used, which otherwise would bring in an additional scaling factor for the mixing rules. A recent paper by Bouazizi and Nasr[32] shows decreasing diffusivity of the ions on increasing LiCl concentration in aqueous solutions due to ion-pairing upto 6 M, however, with much smaller box sizes.

The present work involves MD simulation for the $Li^+.xH_20.yCl^-$ water system to determine the solution phase coordination number of lithium ions in water and, further its effect on Li^+ diffusivity in aqueous solutions at much higher concentrations reaching to 19.28M and larger system size to represent the behaviour of the system very accurately. These studies are expected to provide detail structural as well as energetic information of the solutions of Li salts. Further, we explain in this work, the correlation of diffusion coefficient of different species in the solutions with concentration of LiCl in terms of the clustering of ions and solvent molecules.

2. Methods

The simulation was conducted in a periodic box and 3D periodic boundary conditions were applied.[33] Lithium ions, chloride ions and water molecules were initially distributed randomly in the periodic box. The number of water molecules; lithium cations; and chloride anions in the unit cell were adjusted to represent 0.11 M to 19.28 M salt concentrations. (Table 1)

Table 1: Details of the periodic boxes used for various MD calculations

[LiCl],M	Size of periodic box in nm	Number of Lithium ions	Number of Chloride ions	Number of water molecules
0.11	4.742	7	7	3559
0.22	4.747	14	14	3545
0.346	4.734	22	22	3529
1.268	4.708	78	78	3417
2.362	4.684	140	140	3293
3.364	4.668	193	193	3187
4.52	4.646	250	250	3073
5.90	4.621	313	313	2945
7.01	4.599	360	360	2853
8.01	4.580	400	400	2773
10.11	4.561	477	477	2619
12.03	4.532	540	540	2493
15.73	4.526	646	646	2281
16.87	4.531	675	675	2223
17.89	4.525	700	700	2173
19.28	4.528	732	732	2109

A GROMACS code which integrates Newton's equations of motion for a system of N interacting atoms has been used to perform the MD simulations,[34-36]

$$m_i \frac{\partial^2 r_i}{\partial t^2} = F_i \text{ , i} = 1\ldots\text{N.} \qquad \text{(Eq. 1)}$$

The forces (F_i) are the negative derivatives of a potential function $V\ (r_1, r_2, \ldots, r_n)$:

$$F_i = -\frac{\partial V}{\partial r_i} \qquad \text{(Eq. 2)}$$

The OPLS-AA parameters for lithium[37] and chloride[38] ions were employed to describe the interactions involved in the mixture with the SPC/E water model.[39] Simulations with TIP4P water model were also done to compare the results obtained by both the water models.[40] The OPLS-AA force field is a combination of electrostatic interactions and Lennard-Jones potential, therefore, also called as modified Lennard-Jones force field and expressed as:[41]

$$\emptyset(r_{ij}) = 4 \in_{ij} \left[\left(\frac{\sigma_{ij}}{r_{ij}} \right)^{12} - \left(\frac{\sigma_{ij}}{r_{ij}} \right)^{6} \right] + \frac{q_i q_j}{r_{ij}} \qquad \text{(Eq. 3)}$$

Where, r_{ij} indicates the distance between particles *i* and *j*, σ and $\in$ denote the size parameter and energy parameter, respectively, and q_i indicates the charge on the *i*th atom (*or* ion). The parameters of the force field that were used for the simulation are listed in Table 2.

Table 2: Lennard-Jones and Electrostatic Parameters for the Ion and Water Force Field

Group	**charge**	**σ_{LJ} (Å)**	**ε_{LJ} (kcal/mol)**
OPLS (Li^+)[37]	+1	1.506	0.166
OPLS (Cl^-)[38]	-1	4.02	0.71
SPC/E (H_2O)[39]	+0.4238/-0.8476	3.166	0.650
TIP4P (H_2O)[40]	+0.52/-1.04	3.15369	0.6480

Lorentz Berthelot (LB) mixing rules were used to define the potential parameters for unlike site pairs and expressed as:

$$\sigma_{ij} = \frac{\sigma_i + \sigma_j}{2} \qquad \text{(Eq. 4)}$$

$$\epsilon_{ij} = \sqrt{\epsilon_i \epsilon_j} \qquad \text{(Eq. 5)}$$

A cut off distance of 10 Å was used for the interaction potential and immediate neighbour's list was updated at every fifth time step. The long range electrostatic interactions beyond the cut off distance of 10 Å are treated by particle mesh Ewald method.[41,42] In the simulation, the time steps for the integration, temperature coupling and pressure coupling are 2.0 *fs*, 0.1 *ps* and 2.0 *ps,* respectively.

Energy minimization of the system (below 1000 kJ.mol^{-1}.nm^{-1}) was done by using steepest descent and conjugated gradient algorithms. After the energy minimization, a series of system equilibration runs were performed. At the first instance, the equilibration of the system under an NVT ensemble was conducted for 100 *ps* to stabilize the temperature of system at 300 K with position constraints. The next step of equilibration of pressure was conducted under an *NPT* ensemble for 100 *ps* with position restraints. The system gets well-equilibrated at the desired temperature and pressure after the equilibration phases, so position restraints were released and the production MD run was performed for 1 *ns* for the molecular dynamic trajectory.

The geometry was analyzed for radial distribution function and coordination number as structural parameters. The radial distribution function (RDF) measures the probability of presence of a given atom α at the origin of a random reference frame and another atom β located in a spherical shell of infinitesimal thickness at a distance, r, from the reference atom. The resulting function $g_{\alpha\beta}(r)$, is defined by Hansen and McDonald[43]as:

$$x_\alpha x_\beta \rho g_{\alpha\beta}(r) = \frac{1}{N}\left\langle \sum_{i=1}^{N_\alpha}\sum_{j=1}^{N_\beta}{}' \delta(r - r_i - r_j) \right\rangle \qquad \text{(Eq. 6)}$$

Where, x_i is the mole fraction of chemical type i, N_i is the number of atoms of chemical type i, N is the total number of atoms, and ρ is the overall number density. The prime indicates that the terms where $i = j$ are excluded when the chemical types are the same. The composition of the first coordination sphere of the metal ions in solutions can be determined from the radial distribution function (RDF) against radial distance r.

The average coordination number, $n_{\alpha\beta}$, is defined as the number of atoms of type β present in a spherical shell of thickness dr, at a distance r from atom of type α. The average coordination number $n_{\alpha\beta}$ can be calculated by integrating $g_{\alpha\beta}(r)$ with respect to r as:[43]

$$n_{\alpha\beta} = \rho_\beta \int_0^r g_{\alpha\beta}(r).r^2.dr \qquad \text{(Eq.7)}$$

Where, ρ_β is the number density of atom type β. The radial distribution function, $g_{\alpha\beta}(r)$ is used for the calculation of the coordination number in the solution.

Mean square displacement (MSD) function was used to calculate the dynamic properties of various components. The mean square displacement (MSD) can be calculated[33,44,45] by using Eq.(8)

$$D_i = \lim_{t\to\infty} \frac{1}{6}\langle [r_i(t) - r_i(0)]^2 \rangle \qquad \text{Eq. (8)}$$

where $r_i(t)$ indicates the position of a particle i at time t. In theory, diffusion coefficients or diffusivity (D) of various atom types can be calculated from the slope of the MSD plots, these slopes can be directly related to the molecular diffusion rate, steeper is the slope, higher is the rate of diffusion.[46]

3. Results and Discussion

The MD simulation results have been analyzed at 298 K for the dynamic properties, structural properties and clusterization or aggregation effect on the system properties and are discussed separately.

Structural Properties:

Radial distribution function (RDF) and coordination number (CN) function obtained by the MD simulations are useful for identifying the local structures in the solutions. To get a clear picture of coordination structure, a specimen RDF plot for 10.12 M LiCl concentration is shown in Figure 1. RDF plots of other concentrations are provided in the *supporting information*. The gross features of the structural arrangement of the water molecules around Li^+ ion can be illustrated by the lithium ion-oxygen and lithium ion -chloride ion partial RDFs $g_{Li\text{-}O}(r)$ and $g_{Li\text{-}Cl}(r)$. The patterns of sharp peaks separated by deep minima indicate that relatively stable coordination shells of water molecules and chloride ion exist in these systems. The scrutiny of various shells surrounding the ions depends on the interpretation of the first and the second solvation shells' radii. For both Li-O and Li-Cl pair correlations, the 1st peak is more intense than the 2nd peak and we have also observed that the peak height decreases with increase in the ionic concentration (Figure 2). According to Aragones *et al.*[30], the normal LB rule shows an increase in the intensity of peaks with increasing salt concentration and the 1st peak is less intense than the second one, which was in disagreement with the experimental[31] RDF data, obtained by pair correlation functions. Hence, they have used the modified mixing rules using scaling factors to show this decrease in intensity of peak with increasing concentration and also the greater intensity of 1st peak than the second one. But our calculations show a good agreement with the experimental[31] data with appropriate force field parameters without any modifications of the mixing rules. The Li-Li and Cl-Cl RDFs, as shown in Figures 3 and 4, using standard mixing rules are similar to those reported by Aragones *et al.*[30] Figures 3 and 4 show the pre-peak appearing at 0.38 nm for both Li-Li and Cl-Cl RDFs, the intensity of which increases with increase in LiCl concentration.

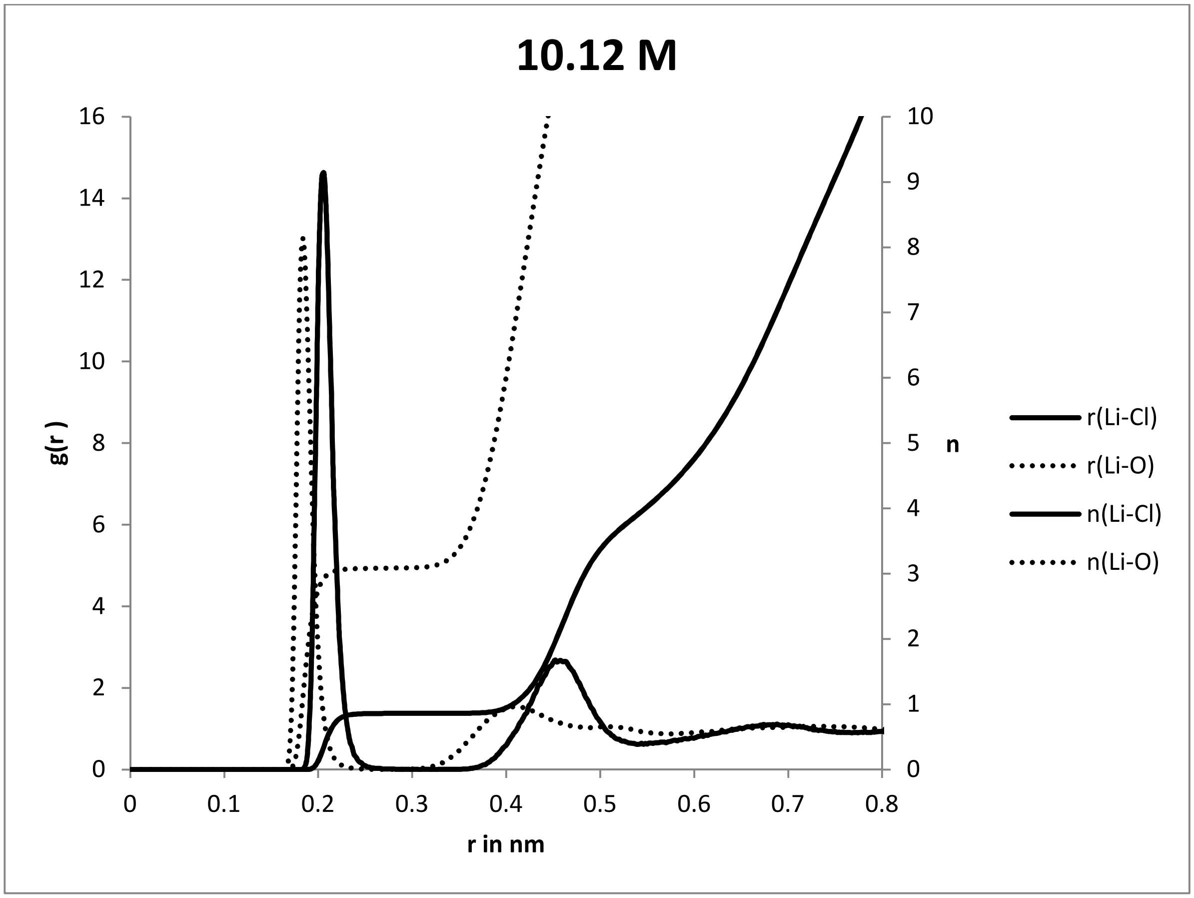

Figure 1: Radial Distribution Functions for 10.12 M LiCl solution

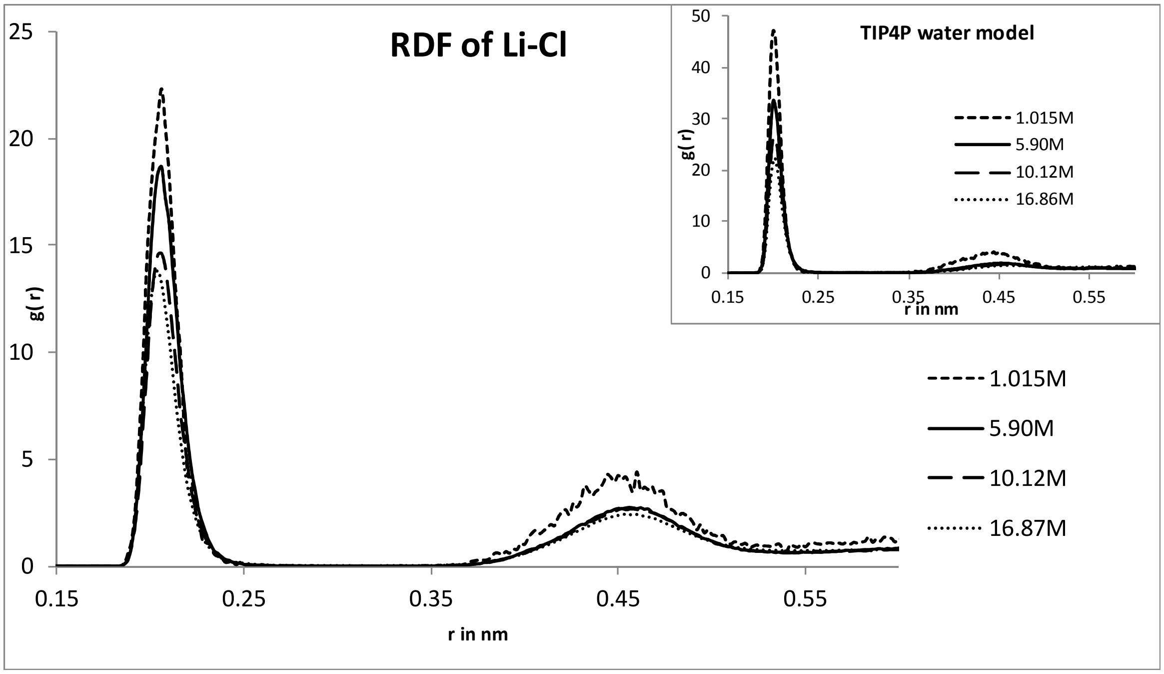

Figure 2. Li-Cl Radial Distribution Function as a function of salt concentration

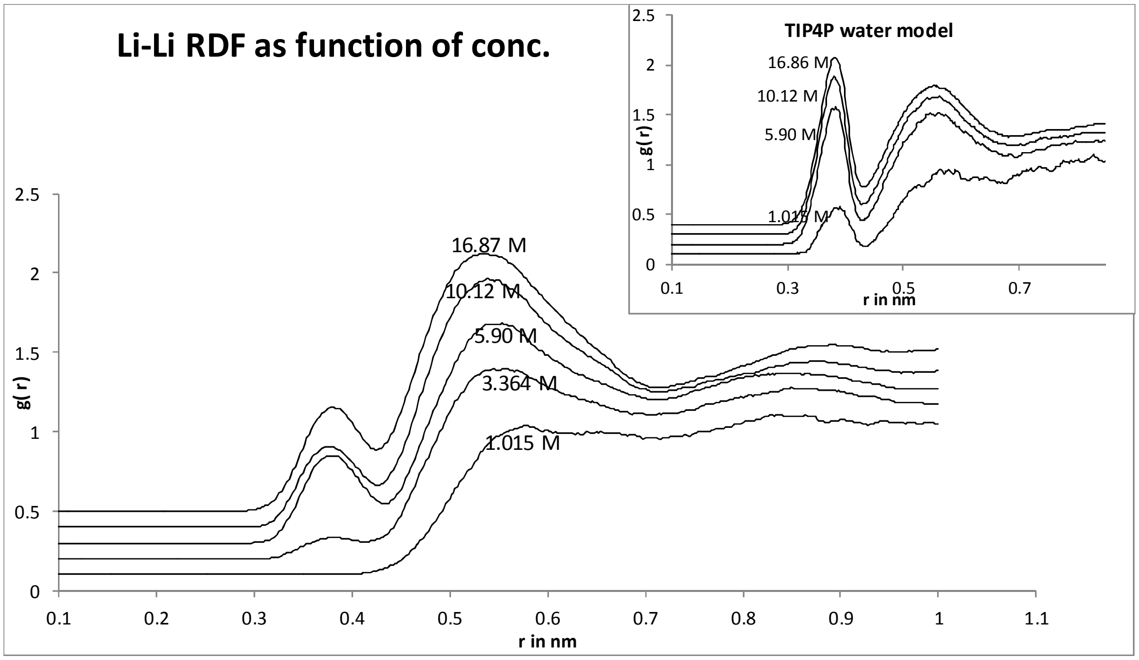

Figure 3: Li-Li Radial Distribution Function plot for different salt Concentration. Every curve is shifted by 0.1 in vertical direction from previous one for clarity**.**

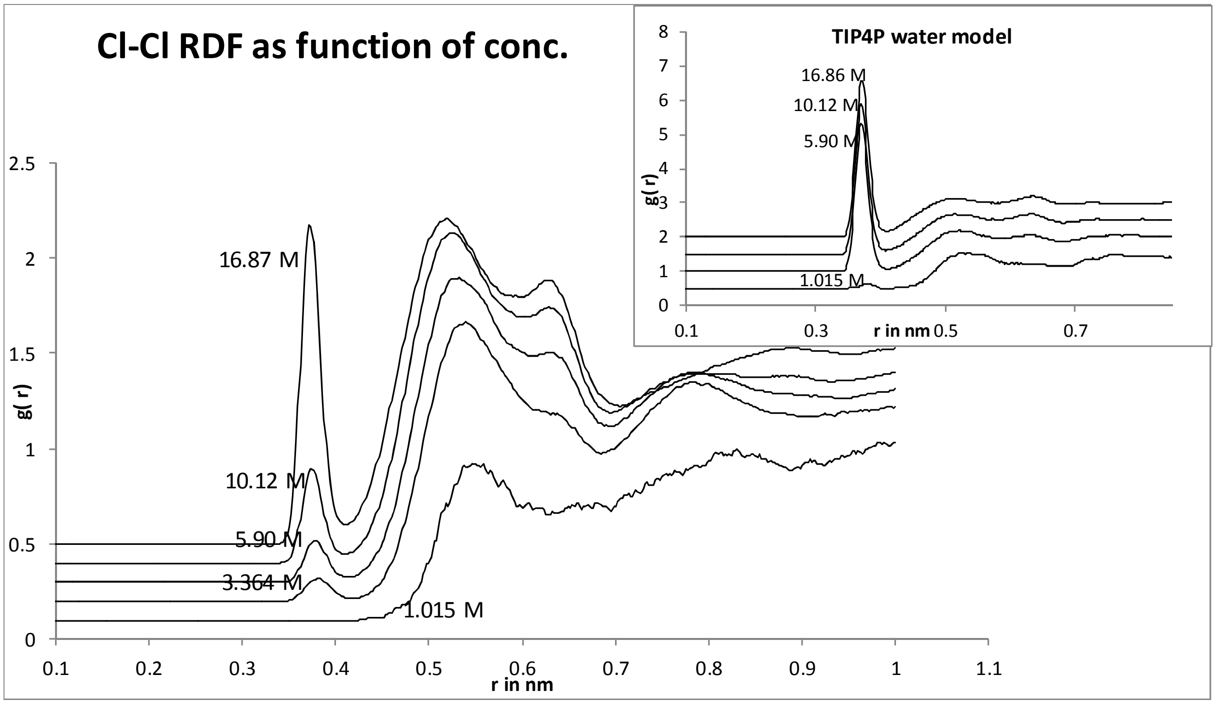

Figure 4:Cl-Cl Radial Distribution Function plot for different LiCl concentrations. Every curve is shifted by 0.1 in vertical direction from previous one for clarity.

The RDF plots clearly show that in the system, Li^+ ions have the most stable and well-defined coordination spheres. Total coordination number of Li^+ ion is four, with the nearest neighbours at ~0.19 nm for Li-O and ~ 0.21 nm for Li-Cl distances. These distances are in good agreement with the experimental values obtained by X-ray and neutron diffraction on the aqueous solutions which are considered to be most reliable(*see Table 3*).[48-50] The X-ray diffraction and neutron diffraction studies reported by Chandrasekhar *et al.*[11] show the hydration shell surrounding of the Li^+ ion to be tetrahedral with the coordination number of 4 and the Li-O distance is between 0.195-0.210 nm by both the techniques and the values are in agreement with our results. We have also observed that, with the increase of lithium chloride concentration (0.11M to 19.28M) in solution, there is slight decrease in the coordination number of Li^+ ions from 3.97 to 3.57 (see

Table 4). This is because at higher concentrations of LiCl, some Li^+ ions coordinate with two chloride ions simultaneously and then only one more water molecule can participate in the 1st coordination sphere of Li^+ ion due to the bulky size of chloride ions, which results in the formation of complexes having Li^+ ion of coordination number 3 and when the number of such Li^+ ions increases in solution, the average coordination number of Li^+ ions decreases.

Table 3: Coordination number of Lithiun ion in aqueous solutions of lithium chloride by (A) X-ray diffraction, (B) Neutron diffraction

[LiCl],M	*r*, nm	Coordination number of lithium ion	Method
1	0.190	4	B[41]
6.9	0.195	4	A + B[47]
6.9	0.195	4	A[48]
9.3	0.202	4	B[49]
9.95	0.195	3.3	B[50]

The hydrogen bonding between the water molecules and interaction with ions explain the number of water molecules in the 1st and 2nd coordination shells of the lithium ion.[51-54] Two water molecules can only form hydrogen bond with each other if the distance between the two interacting atoms is less than 3·5 Å and at the same time H-O distance should be less than 2·45 Å and the O–O–H bond angle should be less than 45°.[53] A chloride ion can only form hydrogen bond with a water molecule if the distance between chloride ion and oxygen is less than 3·90 Å and at the same time H–Cl$^-$ ion distance is less than 3·05 Å and the Cl–O–H bond angle is less than 45°.[55] Table 4 gives the number of chloride ions and water molecules in the first and second coordination shells of lithium for various concentrations of lithium chloride. The number of species in the 1st coordination shell is calculated with the help of radial distribution plots obtained from Equation (2).

As the concentration of salt increases, the number of water molecules in the 1st coordination sphere of lithium ions decreases monotonically. Lithium ion has a very small size; therefore, it generates large local electric field that helps in holding the water molecules tightly in a tetrahedral geometry.

As the concentration of solution increases, negatively charged Cl$^-$ ions start replacing the water molecules from the coordination shell of Li+ ion, and hence the Li$^+$-O coordination number decreases. A Li$^+$ ion coordinates with three water molecules and one chloride ion in the concentration range of 2.36-8.01 M of lithium chloride in water. The same has also been found from the gas phase micro-solvation studies based on Density Functional Theory(DFT).[56] The primary and secondary coordination numbers of lithium ion with respect to the chloride ion increase with the increase in lithium chloride concentration as shown in Table 4. There is significant increase in the secondary coordination number of Li$^+$ ions as compared to primary coordination number because the interaction between the hydrated ions is much more intense than the naked ion-ion interaction.

Table 4: Number of chloride ions and water molecules in the first and the second coordination shells of lithium for various concentrations of lithium chloride

Sr. No.	]LiCl], M	No. of water in the 1st shell	No. of chloride ion in the 1st shell	Coordination number for 1st shell	No. of water in 2nd shell	No. of chloride ion in 2nd shell	Coordination number for 2nd shell
1	0.11	3.99	0	3.99	~9	~0	~9
2	0.22	3.95	0.033	3.983	~9	~0	~9
3	0.346	3.94	0.040	3.98	~8	~0	~8
4	1.268	3.884	0.096	3.98	~7	~1	~8
5	2.362	3.37	0.124	3.98	~7	~1	~8
6	3.364	3.529	0.432	3.961	~10	~1	~11
7	4.52	3.38	0.579	3.959	~7	~3	~10
8	5.90	3.282	0.672	3.954	Aggregation of 2 Lithium ions in a complex		
9	7.01	3.262	0.682	3.944	Aggregation of 2 Lithium ions in a complex		
10	8.01	3.108	0.813	3.921	Aggregation of 2 Lithium ions in a complex		
11	10.12	3.065	0.856	3.921	Aggregation of 2 Lithium ions in a complex		
12	12.03	2.90	0.955	3.855	Aggregation of 2 Lithium ions in a complex		
13	15.730	2.599	1.139	3.738	Aggregation of 2 Lithium ions in a complex		
14	16.867	2.56	1.143	3.70	Aggregation of 2 Lithium ions in a complex		
15	17.89	2.46	1.212	3.67	Aggregation of 4 Lithium ions in a complex		
16	19.28	2.28	1.28	3.57	Aggregation of 5 Lithium ions in a complex		

.

Clustering/ Aggregation Effect

Figure 5 shows that for lower concentrations of LiCl, i.e. less than 1.0 M, the 1st and 2nd hydration shells of Li^+ ion consist only of water molecules. For 2.36 M LiCl concentration, two major types of species are seen in the aqueous solutions. For most of the Li^+ ions, the Cl^- ion is present in only in the 2nd coordination shell, while only few Li^+ ions (24%) have Cl^- ion present in the 1st coordination shell. A clear ion pairing effect is observed for the concentrations ranging from 2.36 M to 4.52 M, i.e. 25-56% ion of Li^+ is paired with one Cl^- ion in the solution. The 1st hydration shell of the Li^+ ion then consists of one Cl^- ion and three water molecules. Similar observations were reported by Chan and Pappu[57] and Hassan[58] for the ion pairing of other alkali metal ions at similar concentrations.

For the salt concentrations at and above 1.39 M, first ion pairing of cation and anion and later clusterization of more ions in the aqueous phase is observed (Table 5). The number of ion pairs or clusters and size of the clusters, in the given volume of the solution, increase with the increase in salt concentration. The size of the cluster is considered in terms of number of Li-Cl ion pairs present in continuation as if in a linear complexation. For LiCl concentrations from 1.39 M to 8.01 M, the size of cluster remains mostly the same i.e. in dimer form as Li^+-Cl^--Li^+, while the number of species forming the cluster increases. For 10.12 M concentration, formation of trimer species, i.e. Li^+-Cl^--Li^+-Cl^--Li^+ is observed, while for 12.03 M to 15.73 M LiCl concentration tertramer species starts appearing in addition to dimer and trimer species. For 16.86 M – 19.28 M LiCl concentration, a population of clusters containing dimers to pentamers and even a few hexamer species of Li-Cl, is observed. The complete cluster analysis for all the concentrations of LiCl is presented in Table 5. As the concentration of LiCl is increased from 1.27 M to 19.28 M, the percentage of Li^+ ions occurring in the cluster form increases from 18% to 97%, respectively.

Table 5: Cluster analysis of Li^+ ions with respect to concentration of LiCl salt

[LiCl], M	% of single ion pair	% of dimer	% of trimer	% of tetramer	% of pentamer	% of hexamer	Total % of clusterization
1.268	18.2	-	-	-	-	-	18.2
2.362	23.5	1.4	-	-	-	-	25.0
3.364	34.7	3.1	-	-	-	-	37.8
4.52	44.4	12.0	-	-	-	-	56.4
5.90	44.7	15.9	-	-	-	-	60.7
7.01	51.9	12.8	-	-	-	-	64.7
8.01	49.0	23.5	-	-	-	-	72.8
10.11	46.9	27.3	1.9	-	-	-	76.1
12.03	50.6	28.9	2.2	-	-	-	82.4
15.73	37.9	43.3	9.3	0.6	-	-	91.1
16.87	39.9	44.6	6.5	1.2	1.6	-	93.8
17.89	36.1	45.7	8.1	3.4	2.1	-	95.6
19.28	29.8	49.6	12.3	3.3	1.4	0.8	97.1

In Figure 6, the estimated density of lithium chloride solutions from the simulation is plotted as a function of salt concentration in the aqueous solution and compared with experimental density values[59] and the simulated values reported by Aragones *et al.*[30] The density values, calculated by simulation using SPC/E water model, are accurate upto 4.52 M LiCl. But as the concentration increases (5.9 M -10.0 M), the deviation of the predicted density from experimental values increases. This can be easily explained by the clusters or aggregates formed in the solution. The percent of clusterization increased upto 61% for 5.9 M and to 97% for 19.28 M concentration of LiCl (Table 5). As the size and number of clusters increases the density of solution increases too. The density values calculated by using the TIP4P water model are also closer to the experimental density values[59] as shown in Figure 6, but the density values calculated by Aragones *et al.*[30] showed significant deviation from the experimental values.

Dynamic Properties:

The MD simulation provides information of time dependent behavior of each participating species in the system. The MSD upto 1 *ns* of different LiCl concentrations were plotted against time. The simulation time of the molecular dynamics, in the present work, was long enough and the slope of the MSD as a function of time was close to unity. The MSD curve was used to estimate the diffusion coefficients (*D*). The estimated diffusion coefficients of water molecules, Li^+ ions and Cl^- ions, for the LiCl concentration of 0.11 - 19.18 M, are in the range of 2.68 - 0.28 x 10^{-9} m^2/s, 1.12 - 0.13 x 10^{-9} m^2/s and 1.95 - 0.13 x10^{-9} m^2/s, respectively, which are in good agreement with the experimental values,[60] validating the simulation. The diffusion coefficient (1.23 - 0.08 x 10^{-9} m^2/s) of LiCl together as a molecule has also been calculated in the above concentration range and shows a very good agreement when compared with the experimental diffusion coefficients in the concentration range of 2.36 - 15.33 M.[61] The diffusion coefficient values obtained by using TIP4P water model also have been compared with the experimental values (Figure 7).

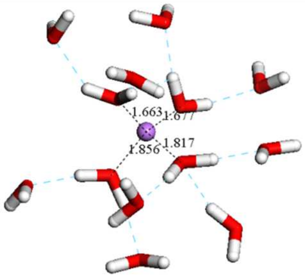

A) 0.11 M

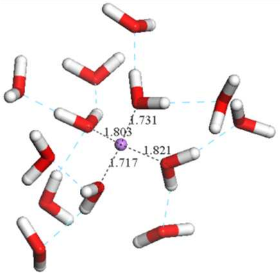

B) 0.22 M

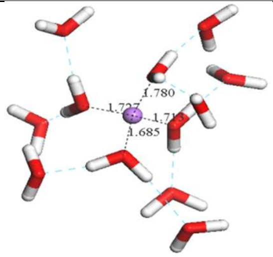

C) 0.346 M

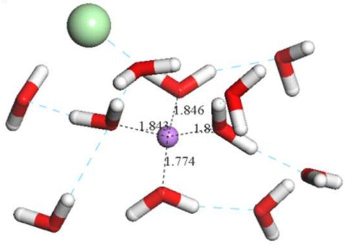

D) 1.268 M

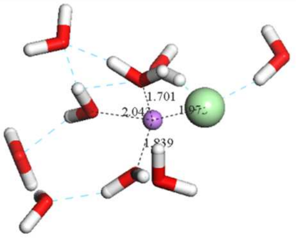

E) 2.362 M (I)

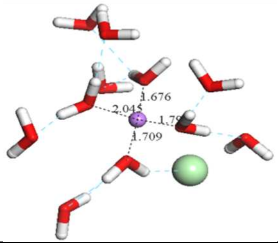

F) 2.362 (II)

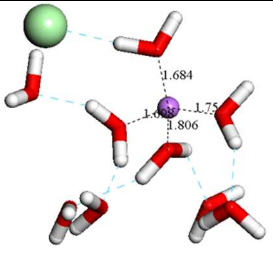

G) 3.364 M (I)

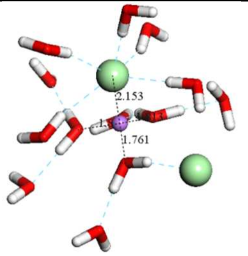

H) 3.364 M (II)

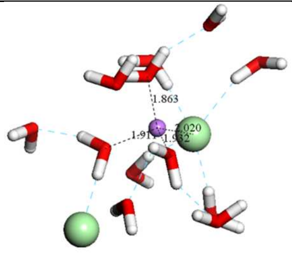

I) 4.52 M (I)

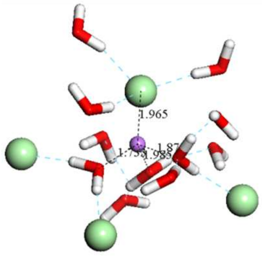

J) 4.52 M (II)

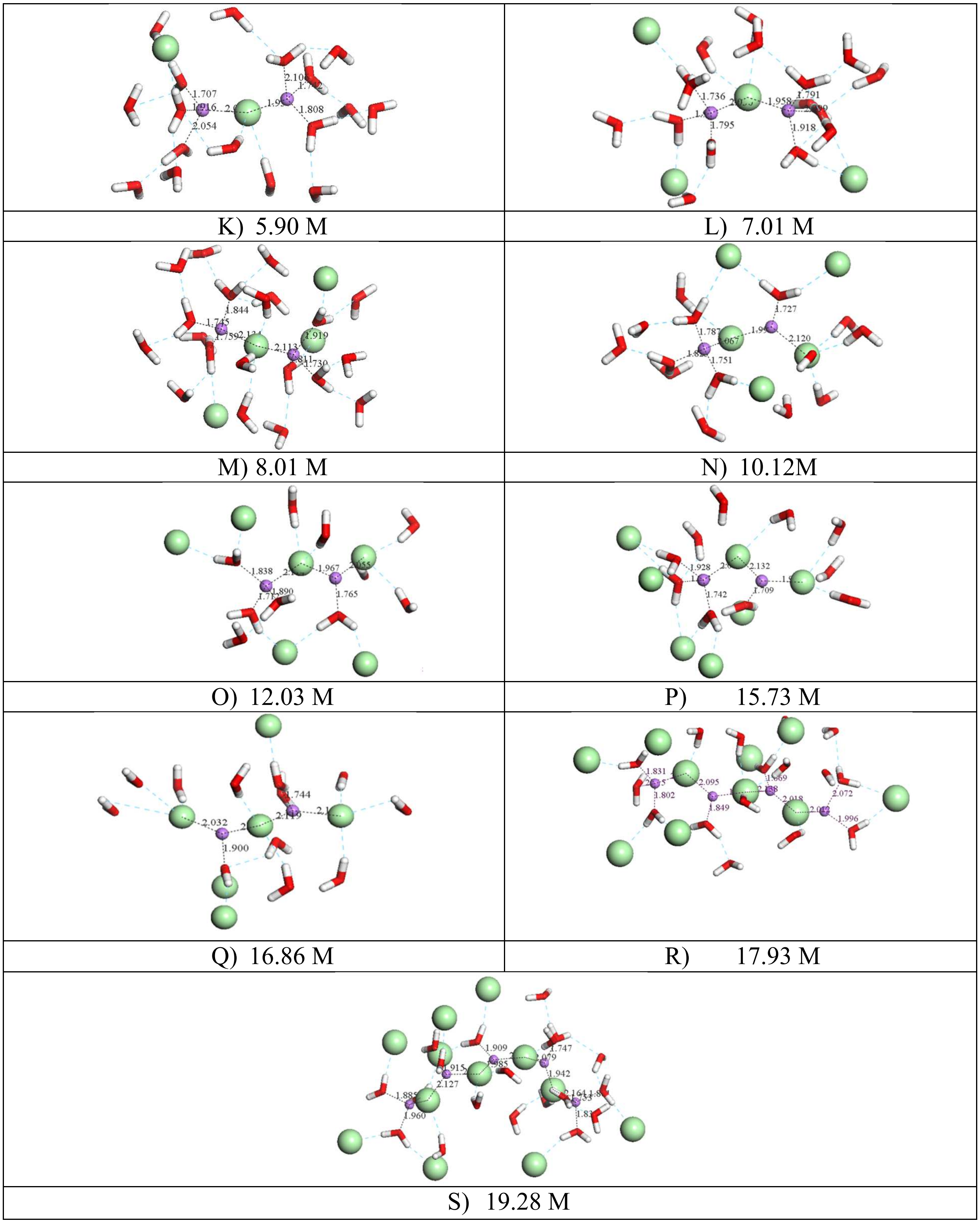

K) 5.90 M

L) 7.01 M

M) 8.01 M

N) 10.12M

O) 12.03 M

P) 15.73 M

Q) 16.86 M

R) 17.93 M

S) 19.28 M

Figure 5: Coordination structures of LiCl at various concentrations in water

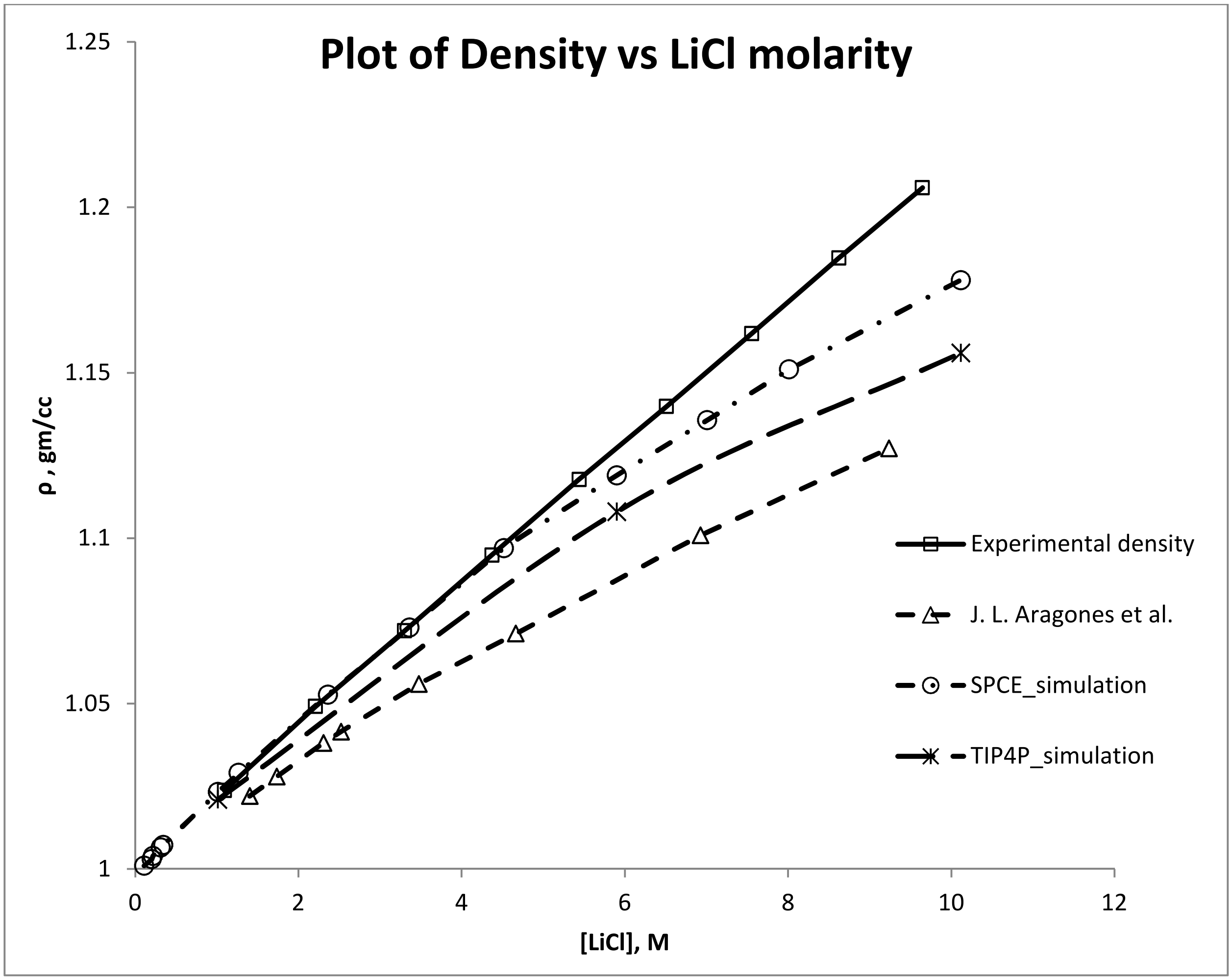

Figure 6: Estimated density of lithium chloride solutions by SPC/E water model in comparison with experimental density[59] and density predicted by Aragones *et al.*[30]

The diffusion coefficients for water molecules, Li^+ ions and Cl^- ions from current work and the literature values,[60] are plotted as a function of LiCl concentration in Figure 7. The figure shows that the diffusivities of Li^+ ions, Cl^- ions and water molecules decrease with the increase in salt concentration. This can be explained in terms of the size of coordination complex or cluster/ aggregate formed by the cation and anions in the salt solution, as discussed earlier. The increased size of complex decreases its movement in a given time interval because when Li^+ ions, Cl^- ions and water molecules are present in the cluster they do not diffuse as individual entities, but as a whole cluster and hence the diffusion coefficient of the involved species decreases. At lower concentrations (0.11-0.346 M), there are basically 13 water molecules including both primary and secondary coordination spheres in the local structure. As the salt concentration increases in the solution (1.268 – 8.01 M), chloride ion becomes part of the primary and secondary coordination spheres resulting in an increased size of the coordination structure. When one Cl^- ion is present in the 1st tetrahedral hydration shell of lithium ion, the distance between the chloride ion and the 'O' of water molecules is 3.4 Å,[27] which is very close to the distance of Cl-O as shown in Figure 8. Thus, these water molecules also participate in the hydration shell of the chloride ion. These water molecules which are both shared by primary coordination shell of lithium ion as well as that of the chloride ion, stick more strongly to Li^+ ion and hence diffusion coefficient of Li^+ ions decreases. For the concentration of LiCl, in the range of 2.36 M to 10.12 M, formation of a small number of clusters or aggregation of 2-3 pairs of Li^+ and Cl^- ions are observed. At very high concentrations of lithium chloride (12.03M - 19.28M), the ions start forming clusters or aggregates containing long chains of –Li^----Cl^----Li^----Cl^---, forming much bulkier complexes. Overall, the simulated diffusion coefficients in solutions appear reasonable relative to the empirically estimated values. An increased size thus reduces the motion and diffusivity of the Li^+ ions in the solution. At lower concentrations of LiCl, the individually hydrated ions tend to move swiftly because primary cation-water interactions are much weaker. The cation-anion interaction becomes prominent at higher concentrations of LiCl. Therefore, increased Van der Walls forces and ion-dipole attraction between cation and water molecules and strong ionic interactions between cations and ions in the cluster decrease the diffusivity at higher salt concentrations.

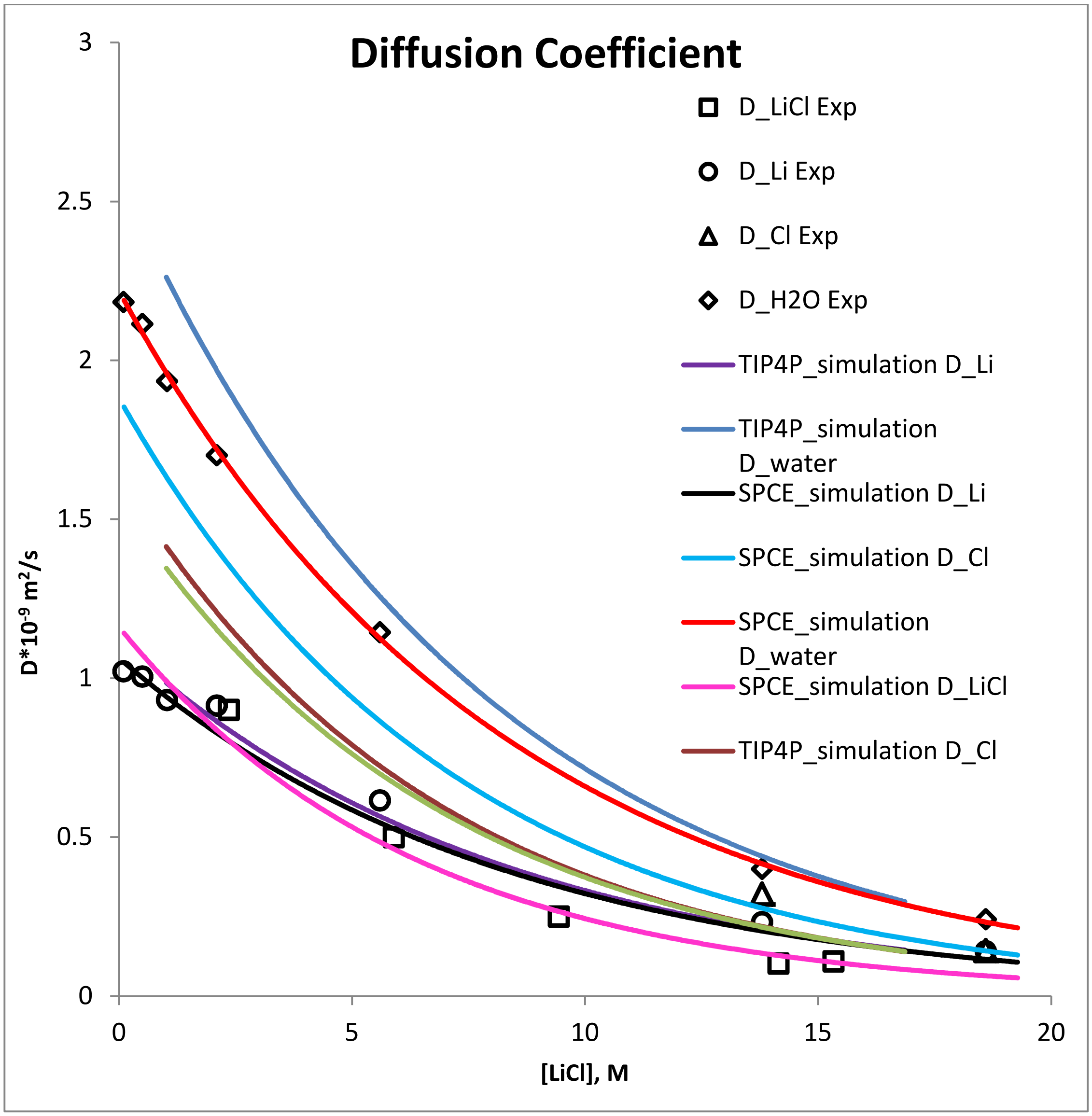

Figure 7: Diffusion coefficients of LiCl molecules, Li^+ ions, Cl^- ions and water molecules in aqueous solutions are plotted as a function of salt concentration. Line represents the trend of diffusion coefficient with respect to salt concentration predicted by MD simulation and hollow symbols represent the experimental diffusion coefficient values of LiCl[61], Li^+ ions, Cl^- ions and water molecules taken from literature.[60]

The predicted Diffusion coefficient data were fitted in an exponential dependence of diffusivity on concentration, i,e., $D(c)=D_o exp(-kc)$ and extrapolated to estimate infinite dilution diffusivity (D_o) of the ions and molecules. The D_o values for Li$^+$ ion, Cl$^-$ ion, LiCl and water molecules are 1.067 X 10^{-9} m^2/s, 1.882 X 10^{-9} m^2/s, 1.162 X 10^{-9} m^2/s and 2.218 X 10^{-9} m^2/s, respectively, which are in good agreement with the diffusivity at infinite dilution values, i.e., D_{o,Li^+}= 1.22 X 10^{-9} m^2/s and D_{o, Cl^-} = 1.77 X 10^{-9} m^2/s, reported in literature.[27]

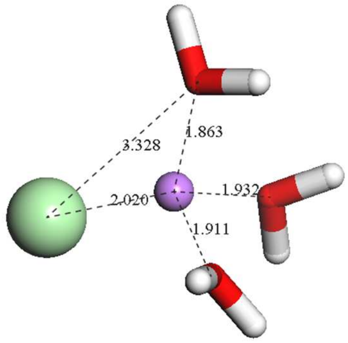

Figure 8: Primary coordination shell structure of Li$^+$ ion, in which one water molecule is replaced by the Cl$^-$ ion. The water molecules are within the distance of primary hydration shell of Cl$^-$ ion.

Diffusion coefficient of Li$^+$ ions is compared with the diffusion coefficients of other alkali metal ions in water for 0.2 M salt concentration in Table 6.[13] Diffusion coefficient values of the metal ions follow the order of Li$^+$< Na$^+$< Cs$^+$< K$^+$< Rb$^+$. This effect can be explained on the basis of the size of ion and its charge density. As the ionic radius of alkali metal ion increases, the diffusion coefficient also increases. Li$^+$ ion interacts strongly with water molecules due to its smaller size and highest charge density and, therefore, restricts the movement of water, while the larger alkali ions such as Cs$^+$, Na$^+$, K$^+$ and Rb$^+$ have ionic size larger than Li$^+$ and have low charge density, therefore, interact weakly with water allowing more free movement of and in water and hence have higher diffusion coefficients.

Extraction of lithium has a great importance, due to its emerging importance in lithium batteries. Generally lithium is extracted from sea water or salty lake brines.[62] But due to presence of other ions, such as sodium and potassium, extraction procedure becomes more complicated. The extraction of lithium from natural resources or exhaust materials is generally based on membrane separation techniques.[62]

Table 6: Diffusion Coefficient of Alkali metal ions in water for 0.2 M salt concentration

Sr. No	Metal Ion	D x 10^{-9} m^2/s	Reference
1	Li^+	1.11	Current work
2	Li^+	1.18	Li and Rasaiah[13]
3	Na^+	1.22	Li and Rasaiah[13]
4	K^+	2.02	Li and Rasaiah[13]
5	Rb^+	2.11	Li and Rasaiah[13]
6	Cs^+	2.00	Li and Rasaiah[13]

Mostly, 14-crown-4 derivatives having phenolic or carboxyl group are used for extraction of Li^+ ions through membrane.[63] During the extraction of lithium ion through membrane, the concentration of Li^+ ions and Cl^- ions increases near the upstream side of the membrane, which is also known as concentration polarization. As the concentration of ions increases, they start forming clusters or aggregates. This in turn will adversely affect their movement into the membrane phase; reducing the extraction rate. Therefore, this study of cluster/ aggregate formation with respect to concentration may be useful in understanding the rates of extraction of lithium.

4. Conclusion

MD simulation of aqueous solutions of lithium chloride for a wide range of concentration of LiCl (0.11-19.28 M) has provided information about the solvation shell structure and coordination of the lithium ions in the solution with the solvent molecules and ionic species and their dependence on the salt concentration. Lithium ion, due to strong electronegativity, binds with water molecules in tetrahedron conformations at lower concentrations. With increase in salt concentration, the coordination of Cl^- with Li^+ increases gradually. At still higher concentrations, the clustering of cation and anions is seen which decreases diffusion coefficient of the species involved in the aggregate. The comparison of the results of density of LiCl solutions and diffusion coefficient of all species in the solutions show a good agreement with experimental values.

References

1. G. W. Neilson, R. D. Broadbent, I. Howell, and R. H. Tromp, *J. Chem.Soc. Faraday Trans.*, 1993, **89**(16), 2927-2936.
2. H. Ohtaki and T. Radnai, *Chem. Rev.*, 1993, **93**, 1157.
3. Y. Marcus, *Biophys. Chem.*, 1994, **51**, 111.
4. S. H. Li and J. C. Rasaiah, *J. Chem. Phys.*, 1994, **101**, 6964.
5. D. A. Doyle, J. M. Cabral, R. A. Pfuetzner, A. L. Kuo, J. M. Gulbis, S. L.Cohen, B. T.Chait and R.MacKinnon, *Science*, 1998, **280**, 69.
6. P. Ayotte, G. H. Weddle, J. Kim and M. A. Johnson, *J. Am. Chem. Soc.*, 1998, **120**, 12361.
7. L. Guidoni, V. Torre and P. Carloni, *Biochemistry*, 1999, **38**, 8599.
8. M. F. Kropman and H. J. Bakker, *Science*, 2001, **291**, 2118.
9. Z. S. Nickolov and J. D. Miller, *J. Colloid Interface Sci.*, 2005, **287**, 572.
10. J. J. Max and C. Chapados, *J. Chem. Phys.*, 2001, **115**, 2664.
11. J. Chandrasekhar, D. C. Spellmeyer, and W. L. Jorgensen, *J. Am. Chem. Soc.*, 1984, **106**, 903.
12. M. Migliore, G. Corongiu, E. Clementi, and G. C. Lie, *J. Chem. Phys.*, 1988, **88**, 7766.
13. S. H. Li and J. C. Rasaiah, *J. Phys. Chem.*, 1996, **100**, 1420.
14. W. Rudolph, M. H. Brooker, and C. C. Pye, *J. Phys. Chem.*, 1995, **99**, 3793.
15. A. K. Soper, *J. Phys.: Condens. Matter*, 1997, **9**, 2717.
16. J. E. Enderby, S. Cummings, G. J. Herdman, G. W. Neilson, P. S. Salmon and N. Skipper, *J. Phys. Chem.*, 1987, **91**, 5851.
17. J. E. Enderby, *NATO ASI Ser., Ser. C*, 1987, **205**, 129.

18. M. Yamagami, H. Wakita, T. Yamaguchi, *J. Chem. Phys.*, 1995, **103**, 8174.
19. E. V. Vinogradov, P. R. Smirnov and V. N. Trostin, *Russian Chemical Bulletin*, 2003, **52**(6), 1253—1271.
20. R. D. Shannon, *Acta Cryst.*, 1976,**A32**, 751-767.
21. F. T. Gucker, D. Stubley and D. J. Hill, *J. Chem. Thermodyn.*, 1977, **9**, 987-989.
22. R. G. Bryant, *Annu. Rev. Biophys. Biomol. Struct.*, 1996, **25**, 29.
23. P. R. Smirnov and V. N. Trostin, *Russian J. General Chem.*, 2006, **76** (2), 175-182.
24. I. S. Joung and T. E. Cheatham, III, *J. Phys. Chem. B,* 2008, **112***,* 9020–9041
25. K. P. Jensen and W. L. Jorgensen, *J. Chem. Theory Comput.*, 2006, **2**, 1499-1509.
26. I. Takashi; B. Mauro; T. Kiyoyuki**,** *J. Chem. Phys.*, 2007, **126(3)**: 034501
27. H. Du, J. C. Rasaiah, and J. D. Miller, *J. Phys. Chem. B,* 2007**, 111***,* 209-217
28. I. S. Joung and T. E. Cheatham III, *J. Phys. Chem. B,*2009, **113***,* 13279–13290
29. M. Fyta, I. Kalcher, J. Dzubiella, L. Vrbka, and R. R. Netz, *J. Chem. Phys*., 2010, **132**, 02491.
30. J. L. Aragones, M. Rovere, C. Vega, and P. Gallo, *J. Phys. Chem. B*, 2014, **118**, 7680−7691
31. K. Winkel, M. Seidl, T. Loerting, L. E. Bove, S. Imberti, V. Molinero, F. Bruni, R. Mancinelli, and M. A. Ricci, *J. Chem. Phys.*, 2011, **134**, 024515.
32. S. Bouazizi, S. Nasr, *J. Mol. Liquids*, 2014, **197**, 77–83
33. M. P. Allen and D. J. Tildesley, *Computer Simulations of Liquids*; Clarendon: Oxford, 1987.
34. H. J. C. Berendsen, D. van der Spoel, and R. van Drunen, *Comp. Phys. Comm.*, 1995, **91**, 43.

35. E. Lindahl, B. Hess, and D. van der Spoel, *J. Mol. Mod.*, 2001, **7**, 306.

36. H. J. C. Berendsen, J. P. M. Postma, W. F. V. Gusteren, A. Dinola, and J. R. Haak, *J. Phys. Chem.*, 1984, **81**, 3684.

37. X. Li and Z. Yang, *J. Phys. Chem. A*, 2005, **109**, 4102-4111.

38. K. P. Jensen and W. L. Jorgensen, *J. Chem. Theory Comput.*, 2006, **2**, 1499-1509.

39. P. Mark and L. Nilsson, *J. Phys. Chem. A*, 2001, **105**, 9954-9960.

40. M. W. Mahoney and W. L. Jorgensen, *J. Chem. Phys.*,2001, **115**, 10758.

41. T. Darden, D. York, and L. Pedersen*, J. Chem. Phys.*, 1993, **98**, 10089.

42. U. Essmann, L. Perera, M. L. Berkowitz, T. Darden, H. Lee, and L. G. Pedersen, *J. Chem. Phys.*, 1995,**103**, 8577.

43. J. P. Hansen and I. R. McDonald, *Theory of Simple Liquids*, Academic, London, 1986.

44. S. Koneshan, J. C. Rasaiah, R. M. Lynden-Bell and S. H. Lee, *J. Phys. Chem. B*, 1998, **102**, 4193.

45. S. Chowdhuri and A. J. Chandra, *Chem. Phys.*, 2001, **115**, 3732.

46. D. Brandell, H. Kasemägi and A. Aabloo, *Electrochimica Acta*, 2010, **55** (4),333-1337.

47. A. H. Narten, F. Vaslov and H. A. Levy, *J. Chem. Phys.*, 1973, **58**(11), 5017.

48. J. E. Enderby and G. W. Neilson, *In Water -A Comprehensive Treatise*, Volume **6**, ed. F. Franks, Plenum, 1979, Chapter 1.

49. T. Yamaguchi, M. Yamagami, H. Ohzono, K. Yamanaka, and H. Wakita, *Physica (B)*, 1995, **213/214**(1, 4), 480.

50. J. R. Newsome, G. W. Neilson, and J. E. Enderby, *J. Phys. C: Solid State Phys.*, 1980, **13 (32)**, L923.

51. A. Chandra, *J. Phys. Chem.*, 2003, **107**, 3899

52. S. Chowdhury and A. Chandra, *J. Phys. Chem. B*, 2006, **31**, 159.

53. G. Sutmann and R. Vallauri, *J. Phys: Condensed Matter*, 1998, **10**, 9231.

54. A. Luzar and D. Chandler, *Phys. Rev. Lett.*, 1996, **76**, 928; A. Luzar and D. Chandler, *Nature (London)*, 1996,**379**, 53.

55. A. Nag, D. Chakraborty and A. Chandra, *J. Chem. Sci.*, 2008, **120** (1), 71–77

56. K. Yamaji, Y. Makita, H. Watanabe, A. Sonoda, H. Kanoh, T. Hirotsu and K. Ooi, *J. Phys. Chem.*, 2001, **105**, 602–613.

57. A. A. Chen and R. V. Pappu, *J. Phys. Chem. B,* 2007, *111,* 6469-6478.

58. S. A. Hassan, *J. Phys. Chem. B,* 2008, *112,* 10573–10584.

59. E. Vercher, S. Solsona, M. Vazquez, Martinez-Andreu, *Fluid Phase Equilib.*, 2003, **209**, 95-111.

60. K. Tanaka, M. Nomura, *J. Chem. Soc.*, *Faraday Trans. 1*, 1987,**83**, 1779-1782.

61. Personal Communication with Frank Stallmach, Department of Physics, University of Leipzig.

62. T. Hoshino, *Desalination*, 2013, **317**, 11-16

63. T. Araki, H. T Sukube, *Liquid Membranes: Chemical Applications*, CRC Press, Boca Raton, 1990.